AGU ADVANCING EARTH AND SPACE SCIENCE

Geophysical Research Letters®

RESEARCH LETTER
10.1029/2022GL098123

Key Points:

- Hunga Tonga volcanic explosion has been automatically detected with surface waves recorded by global seismological networks
- Analysis of global surface waves resulted in measurement of the explosion impulse and led to estimating its Volcanic Explosivity Index as 6
- With near-real-time implementation of our methods, major volcanic explosions can be detected and characterized within less than 2 hr

Supporting Information:

Supporting Information may be found in the online version of this article.

Correspondence to:

P. Poli,
pieropoli85@gmail.com

Citation:

Poli, P., & Shapiro, N. M. (2022). Rapid characterization of large volcanic eruptions: Measuring the impulse of the Hunga Tonga Ha'apai explosion from teleseismic waves. *Geophysical Research Letters*, *49*, e2022GL098123. https://doi.org/10.1029/2022GL098123

Received 31 JAN 2022
Accepted 28 MAR 2022

Rapid Characterization of Large Volcanic Eruptions: Measuring the Impulse of the Hunga Tonga Ha'apai Explosion From Teleseismic Waves

Piero Poli[1] **and Nikolai M. Shapiro**[1]

[1]ISTerre Institut des Sciences de la Terre, CNRS, Université Grenoble Alpes, Gières, France

Abstract Most of the largest volcanic activity in the world occurs in remote places such as deep oceans or poorly monitored oceanic island arcs. Thus, our capacity of monitoring volcanoes is limited to remote sensing and global geophysical observations. However, the rapid estimation of volcanic eruption parameters is needed for scientific understanding of the eruptive process and rapid hazard estimation. We present a method to rapidly identify large volcanic explosions, based on analysis of seismic data. With this methodology, we promptly detect the 15 January 2022 Hunga Tonga Ha'apai eruption. We then analyze the seismic waves generated by the volcanic explosion and estimate its important first-order parameters. We further relate the parameters with the volcanic explosivity index (VEI). Our estimate of VEI ∼ 6 indicates that how the Hunga Tonga eruption is among the largest volcanic activity ever recorded with modern geophysical instrumentation and can provide new insights into the physics of large eruptions.

Plain Language Summary The Hunga Tonga Ha'apai volcanic eruption that occurred on 15 January 2022 had a global impact by ejecting a huge volume of ashes and volcanic gases in the atmosphere and with generating a tsunami that affected many Pacific countries. This volcanic event has been also well recorded by modern satellite and land-based geophysical instruments. Despite the unprecedented wealth of high quality and rapidly available scientific data, main quantitative parameters of the Hunga Tonga volcanic eruption such as its size in comparison with previous major eruptions could not be estimated rapidly with "standard" monitoring algorithms. This emphasizes the need to develop new approaches for analysis of instrumental observations. We show how the data recorded by seismographic stations operating all around the World, which are available in real time, can be analyzed to determine main eruption parameters including its location and size within less than 2 hr after its occurrence.

1. Introduction

Despite the development of volcano observatories in many of the ∼1,340+ subaerial volcanoes (Global Volcanism Program, 2013), many others (whose exact number is not well defined, www.usgs.gov/faqs/how-many-active-volcanoes-are-there-earth) are in remote place or underwater, and can thus be monitored only with satellite observations (e.g., Vaughan & Webley, 2010) and global networks of geophysical instruments. The recent Hunga Tonga Ha'apai (Hunga Tonga for short) catastrophic eruption perfectly illustrated this situation. This event occurred on 15 January 2022 on a small uninhabited and unmonitored volcanic island. Its impact, however, was truly global. The volcanic explosion ejected an enormous ash plume well recorded by satellites and significantly affecting the Tonga islands, generated a very strong atmospheric pressure wave recorded by meteorological and infrasound sensors across the World, and was followed by a well recorded tsunami that affected many Pacific coastal regions (Duncombe, 2022).

Based on information available today, the Hunga Tonga explosion is most likely to be the largest one occurred in the last 3 decades (Duncombe, 2022), but still, despite the large amount of observations available, a full rapid quantitative estimation of the size of this eruption remains challenging.

Quantifying the size and strength of volcanic eruptions is a difficult task because of their strongly varying styles and poor available data for many past eruptions. The widely used parameter in volcanology is the Volcanic Explosivity Index (VEI) that is computed from estimated ejecta volumes and/or heights of eruptive ash columns and with taking into account the eruption stile and duration (Newhall & Self, 1982). The VEI scale allowed to build a quantitative catalog that includes many historical and pre-historical eruptions (Mason et al., 2004;

Newhall & Self, 1982). Extending this catalog back in time is very important for statistical analysis because of very rare occurrence of largest eruptions (VEI $\geq$ 5). For most of the cataloged eruptions, the VEI has been determined from the estimates of the ejecta volumes while other types of data not being available. Therefore, the VEI can be approximately characterized as a discrete scale generally proportional to the logarithm of the erupted volume (e.g., Pyle, 1995). Main flaws of the VEI scale are its discrete character and the difficulty to estimate from the volume of the deposits its dense rock equivalent that is more directly related to the amount of erupted magmas. Therefore, a continuous eruption magnitude scale determined from the logarithm of ejected mass has been suggested to replace/complement the VEI (Mason et al., 2004; Pyle, 1995).

The VEI scale is also inconvenient from the point of view of real time monitoring because estimating volumes of erupted materials remains relatively slow, as can be seen with the Hunga Tonga eruption. At the same time, today's strong volcanic explosions are recorded by satellites and hundreds of high-quality geophysical instruments distributed all over the World. An efficient usage of these data for global-scale real-time volcanic monitoring requires developing an instrument-based scale of the size of eruptive phenomena, similar to magnitudes or seismic moments routinely determined for earthquakes. Ideally, such a refined "eruption magnitude" scale should be based on a plausible physical model of the eruptive process (source) and could be linked with widely used VEI scale.

Because of the very variable style of volcanic eruptions, a universal physical model of the eruption processes is not possible. Here, we focus on the most dangerous strong explosive eruptions. The waves emitted by these events are well recorded by global networks of seismic and infrasound stations. The latter are particularly energetic because of the strong coupling of volcanic explosions with the atmosphere and, therefore, have been used to model volcanic explosion source process (e.g., Haney et al., 2018; Matoza et al., 2011) and to estimate eruptive volumes (e.g., Fee et al., 2017). Acoustic coupling with the ionosphere also can be used for volcano monitoring (e.g., Manta et al., 2021). One of the main difficulties with the infrasound monitoring of the eruptions is the need to correct non-stationary propagation effects that are strongly dependent on atmospheric winds (e.g., Le Pichon et al., 2005). Atmospheric acoustic waves are also relatively slow, and several hours are required to record a representative dataset from a global network (see Figure S3 in Supporting Information S1).

On the contrary, seismic waves propagation is stable in time and rather fast. Surface waves from large volcanic explosions (and body waves for the strongest ones) are regularly recorded, and data from hundreds of stations can be collected within an hour following the explosion. This makes seismic networks one of the most suitable tools for the near real-time monitoring of volcanic explosions and determining their physical characteristics (e.g., Prejean & Brodsky, 2011; Zobin et al., 2006). At the same time, "standard" seismological methods and metrics developed for earthquake monitoring are not applicable to volcanic explosions. First, the latter do not emit strong high-frequency body waves that are used in most of earthquake detection algorithms. Second, the earthquake magnitude and moment scales are not applicable to volcanic explosions because of different frequency ranges and because of the fundamentally different source mechanism.

In this short paper, we show how a fast analysis based on backprojection of long-period surface waves recorded by the global seismic network (e.g., Ekström, 2006; Poli, 2019) could be used to detect the Hunga Tonga explosion nearly in real time and to determine its geographical location. We then use a model describing the mechanical effect of volcanic eruption as a single force (Kanamori & Given, 1982; Kanamori et al., 1984; Nishimura, 1995) to deconvolve the propagation effect in order to estimate the source force spectra that, in turn, can be used to approximately estimate the overall mechanical impulse of the explosion (Volcanic Explosion Impulse, VEIm) and its duration. We than use the volcanic jet model (Brodsky et al., 1999; Prejean & Brodsky, 2011) to estimate the total ejected mass and link it to the VEI. Overall, the implemented seismic data analysis provides a realistic and physics-based workflow for near real-time monitoring of large volcanic explosions.

1.1. Detection of Long Period Seismic Events

The detection algorithm is similar to Shearer (1994) and Poli (2019), (see also Ekström, 2006) and is based on the analysis of 24 hr seismograms recorded by global seismic networks (Albuquerque Seismological Laboratory (ASL)/USGS, 1988; GEOFON Data Centre, 1993; Institut de physique du globe de Paris (IPGP), École et Observatoire des Sciences de la Terre de Strasbourg (EOST), 1982; Scripps Institution of Oceanography, 1986) shown in Figure 1a. The data are resampled at 0.1 Hz and corrected for the instrumental response. Only long period and

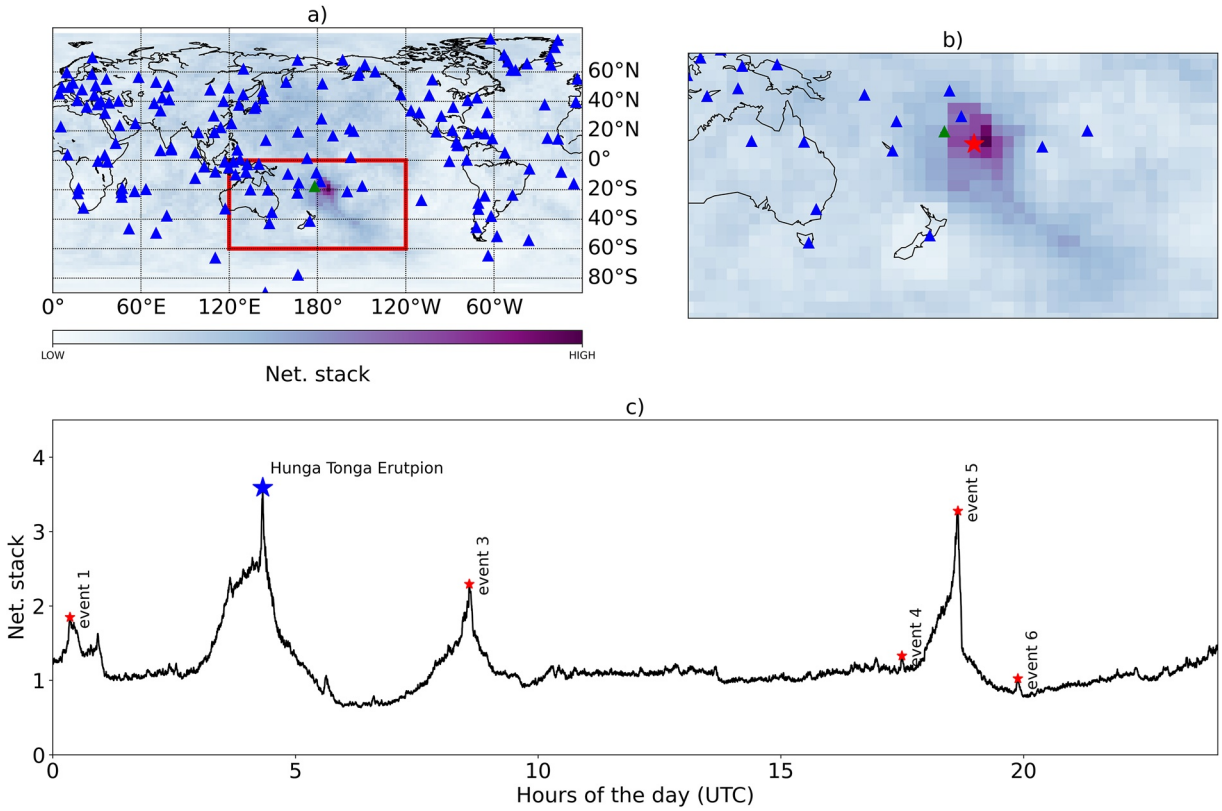

Figure 1. (a) Map showing seismic stations used in this study (blue triangles) and the network stack at the Hunga Tonga event time. The green triangle is a reference station used to plot the spectrum of recorded signal in Figure 2. The red polygon encloses the source region plotted in (b). The red stat in (b) is the position of the Hung Tonga volcano. (c) Network stack for the 15 of January 2022, with detected events represented by red stars. The blue star indicates the detection associated with the Hunga Tonga eruption.

vertical components channels are used (LHZ and VHZ), and data are filtered in between 0.01 and 0.03 Hz. Similar to Shearer (1994), each seismogram is then transformed into STA/LTA time series, using a recurrent scheme (Whiters et al., 1998) with STA = 120 s and LTA = 900. We then assume equally spaced sources every 2.5°, located at the surface of the Earth. For each source, we align the seismograms assuming a velocity of 3.85 km/s, derived from PREM (Dziewonski & Anderson, 1981), and stack all traces. For every time sample, the stacked signal at each source position is saved. The maxima of the stacked signal as function of time define the network stack (Figure 1c), from which we extract events, as local maxima with prominence larger than 0.2 and interspaced by at least 3,600 s. These parameters have been arbitrarily chosen after many tests to minimize the incidence of false detections, while favoring detection of small-sized events.

Detections are associated with known earthquakes, if a seismic event of magnitude larger than 3 (ISC catalog, Storchak et al., 2013) occurs within 10° and 3,600 s from the time and position of our detection. Otherwise, a detection is flagged as a new event. The detection procedure runs automatically every day, at 5 a.m. (UTC+1) on a desktop computer and takes ∼5 min. Every day, an event report is produced with known earthquakes and new detections.

From the time-continuous analysis of long period surface waves described above, we detected a new event, on Saturday 15 of January 2022 (UTC 04 h 16 m 00.07 s), with location close to the Tonga Islands, as showed in the map of back-projected signals in Figures 1a and 1b. This event was rapidly associated with a major volcanic eruption of the Hunga Tonga, announced by many media.

Figures 1a and 1b show the distribution of the network stack for each tested source position at the time of the event (15 of January 2022 UTC 04 h 16 m 00.07 s), with the violet areas representing the most likely location of the discussed event. We observe that the backpropagated energy is spread over an area of ∼5°, which results from the long wavelength of the Rayleigh waves employed and the finiteness (2.5°) of our grid of potential sources.

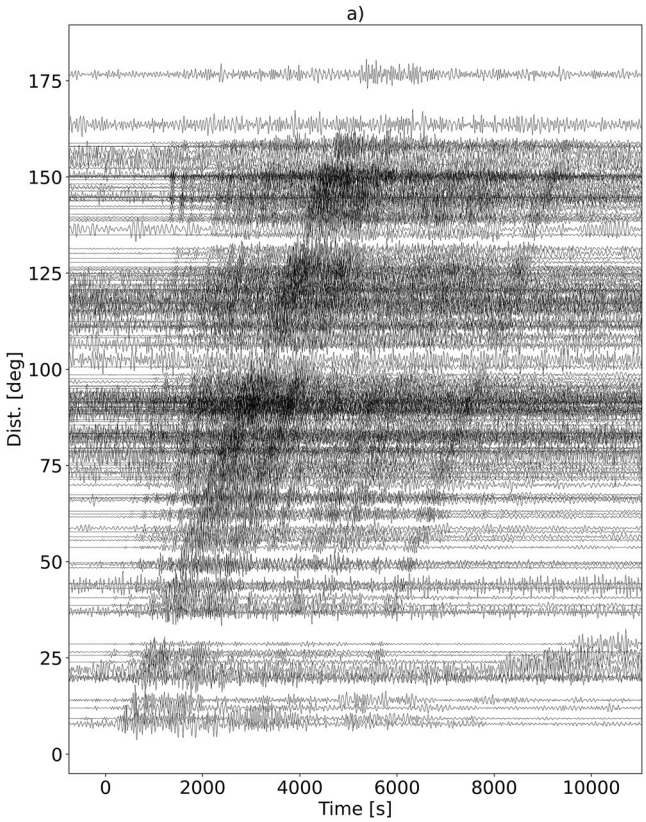

Figure 2. Signals generated by the Hunga Tonga eruption, recorded at stations of the global seismographic network reported in Figure 1a, plotted as function of distance from the source. Each trace is normalized by its absolute maximum and filtered in between 0.01 and 0.04 Hz.

Beyond the Hunga Tonga event, on the 15 of January 2022, five additional detections are present (Figure 1c), three of which are associated with known earthquakes, while the other two are a long period event in the Pacific Antarctic ridge and a possible icequake in East Antarctica (see Supporting Information).

The waveforms for the Hunga Tonga event are plotted in Figure 2 and show a good alignment when ranged as function of distance from the source, proving the quality of our location. The dominant signals are Rayleigh waves (Figure 2), with several impulses, likely to represent explosion episodes, similar to the mount St. Helens eruption in 1980 (Brodsky et al., 1999; Kanamori & Given, 1982). These sequence of explosions make the Rayleigh waves train last for ~6,000 s, a time which can be taken as an approximated estimation of the duration of the eruption. Before the arrival of surface waves, more rapid S and P waves are also observed (Figure 2).

1.2. Impulse of the Explosive Eruption

The seismic radiation of large volcanic explosions can be approximated with a response to a reaction force acting on the ground in the direction opposite to the motion of the ejected ash column (e.g., Cruz-Atienza et al., 2001; Kanamori & Given, 1982; Nishimura, 1995). Therefore, the far-field seismic wavefield can be expressed as a convolution of the single force with the Green's function:

$$u(t,r) = F(t) * G(t - t_s, r, r_s) \tag{1}$$

where $u(t,r)$ is the displacement observed in location r, r_s, and t_s are location and origin time of the explosive eruption, G is the Green's function, and $F(t)$ is time variable force acting as the explosion source. Equation 1 implies that given sufficiently broadband three-component records available at several stations and azimuths, a full vector force time history can be retrieved via convolution or inversion procedures (e.g., Allstadt, 2013; Cruz-Atienza et al., 2001; Kanamori & Given, 1982).

To simplify the rapid data analysis, we consider an approximation of a vertical explosion and force, which is plausible at first order considering the nearly radially symmetric shape of the Hunga Tonga ash cloud seen by satellites. In this case, the vertical displacement can be written as:

$$u_z(t,r) = F_z(t) * G_{zz}(t - t_s, r, r_s) \tag{2}$$

where F_Z is the vertical force and G_{zz} is the vertical component of the Green's function for a vertical force at the source. Again, the full force time history $F_z(t)$ can be retrieved by applying a deconvolution of Equation 2 to the data. The spectral representation of the source force $F_z(\omega)$ is computed with a Fourier transform:

$$F_z(\omega) = \int F_z(t) e^{-i\omega t} dt \tag{3}$$

If the explosion time history $F_z(t)$ is positively defined, its Fourier spectrum $F_z(\omega)$ will converge at low frequencies to a "plateau":

$$\lim_{\omega \to 0} F_z(\omega) = \int F_z(t) dt = K_0 \tag{4}$$

where K_0 is the mechanical impulse of the material ejected by the explosion. If the force can be approximated with a single unidirectional pulse of duration τ_{exp}, the spectral amplitude falls down above the corner frequency f_c approximately inverse to the explosion duration:

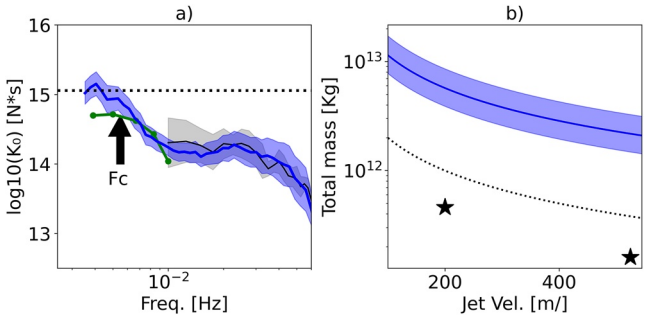

Figure 3. (a) Source spectrum obtained from the deconvolution of 6,000 s of signal containing Rayleigh waves described in Equation 6 (continuous blue line) and its confidence bound (blue area). The black line and gray area show estimated obtained using P waves. The arrow indicates the estimated corner frequency (f_c) and the dashed line shows the estimated VEIm ($K_0 = 1.3 \times 10^{15}$N s). We also report in green the estimated (nearly horizontal) force spectrum for the Mt. St. Helens, 1980 eruption (Kanamori & Given, 1982). (b) Total ejected mass as function of jet velocity (blue line) and its uncertainty (blue area). The stars are the total ejected mass and assumed jet velocity for the 1980 Mt St Helens eruption estimated by Brodsky et al. (1999). The dashed line is the estimated ejected mass using only P waves.

$$f_c \approx 1/\tau_{exp} \tag{5}$$

There is a clear similarity with the low-frequency asymptotic behavior of the classical earthquakes spectra (e.g., Brune, 1970; Kanamori & Given, 1982). The main difference is that the seismic moment M_0 is replaced with the value K_0 (Equation 4) that is equal to the total explosion impulse (e.g., Cruz-Atienza et al., 2001; Nishimura, 1995). Therefore, similar to the analysis of earthquake, two main parameters of volcanic explosion K_0 and f_c can be determined from the analysis of the source amplitude spectra (Kanamori & Given, 1982). This implies that we do not need to compute a full deconvolution of Equation 2 and can use its amplitude version in the Fourier domain:

$$|u_z(\omega)| = |F_z(\omega)||G_{zz}(\omega)| \tag{6}$$

to retrieve the amplitude source spectra $|F_z(\omega)|$ from simple spectral ratios.

To estimate the source spectrum, we use the data shown in Figure 2a. At this stage, we do not down-sample the seismograms and bandpass them between 0.0001 and 0.1 Hz and convert them into displacement by removing the instrument responses. The vertical component Green's functions for a vertical force is obtained from the "syngine" data service (Hutko et al., 2017) based on the PREM model (Dziewonski & Anderson., 1981). We then use Equation 6 and calculate the spectral ratio between the recorded signals and the Green's functions, to estimate the source spectrum $|F_z(\omega)|$ for the Hunga Tonga eruption. The spectral ratios are calculated for each station using the full duration of the eruption that is 6,000 s following the arrival times of Rayleigh waves, calculated from PREM. This window is chosen to avoid interference with the long period and strong amplitude signals, for atmospheric acoustic waves, well recorded by seismic stations (see Figure S3 in Supporting Information S1).

Before calculation of the spectral ratio (Equation 6), we estimate the signals-to-noise ratio (SNR) for each spectrum. The SNR is defined as the ratio of the amplitude spectrum for the surface waves and for 1 hr of signal preceding the eruption. Only frequencies with SNR > 10 are retained for further analysis.

The final force spectrum is the average of single station estimates (blue line Figure 3a), while the data error is the standard deviation of the 41 single station force spectra (blue area, Figure 3a). The force spectrum shows a low frequency spectral "plateau" for frequency lower than 5 mHz, which is used to estimate the explosion impulse (Equation 4): $K_0 \approx 1.3 \times 10^{15}$ Ns. The spectrum starts to fall-off at a corner frequency $f_c \approx 0.005$ Hz, suggesting an approximate explosion duration of ~200 s (Equation 5). We cannot exclude a possibility that the obtained value of K_0 might be underestimated (and f_c overestimated) because of the limited signal-to noise ratio at very low frequencies. These values have therefore to be considered as a lower bound estimates of the full explosion size and duration.

We further estimate the force spectrum for well recorded P waves. We only focus on the frequency range from 0.01 to 0.07 Hz, where signal-to-noise ratio of the P waves is suitable for our analysis. We then isolate 200s of signal, around the P waves arrival time estimated from PREM model (Dziewonski & Anderson, 1981). We use again Equation 6 to estimate the force for the signals recorded at 42 stations. The average force spectrum from P waves (black line in Figure 3a) is remarkably similar to the one from Rayleigh waves at frequencies above 0.01 Hz. We also note that the spectral fall-off above the corner frequency is not "homogeneous" with appearance of a second plateau between 0.01 and 0.04 Hz. This implies that, if we would make "rapid" estimations based on P-waves or on relatively high-frequency Rayleigh waves (as those used for the backprojection shown in Figures 1 and 2) we would obtain $K_0 \approx 2 \times 10^{14}$ Ns and a corner frequency close to 0.04 Hz. This observation with the shape of the amplitude source spectrum (Figure 3a) indicates that the eruption force time function $F(t)$ is most likely composed of several pulses with different durations (which would explain the existence of two spectral plateaus) and that the analysis of only P waves (or band-limited surface waves) does not capture the full impulse of the eruption but only its relatively short-time scale component. However, such analysis can be still useful to

obtain a rapid lower bound estimate of the explosion impulse (Figure 3a) and total ejected mass (dashed black line in Figure 3b).

1.3. Relationship Between the VEIm, the Erupted Mass and Volume, and the VEI

Our analysis suggests that the explosion impulse K_0 is the parameter that can be directly and robustly estimated for large explosive eruptions, from a simple and fast analysis of broadband seismic records. It is also a natural dynamic parameter characterizing the explosions similar to seismic moment characterizing the earthquakes. Therefore, the VEIm could be considered as a cornerstone for building instrument-based scales of the size of volcanic explosions. At the same time, this is important to link this parameter with other existing seismological and volcanological scales.

From a seismological point of view, determinations of K_0 could lead to developing a physical seismic magnitude scale as has been suggested by Cruz-Atienza et al. (2001). Based on analogy with the moment magnitude scale for earthquakes, the relationship between the magnitude M and the explosion impulse could be written as $M = 2/3\log K_0 + C$, where the constant C should be calibrated to approximately fit "standard" magnitude estimations. However, such calibration is beyond the scope of this study.

As described in the introduction, the main scale used in volcanology is the VEI that is a logarithmic scale based on estimations of the erupted volume (Newhall & Self, 1982). The latter can be approximately estimated from the explosion impulse, assuming a value for erupted material density and a simple physical model for the volcanic explosion. In particular, we use the model of Brodsky et al. (1999) in which the reaction force from the explosion is described as a jet force F_{jet}. For simplification, we consider an explosion with a constant jet velocity v_{jet}, leading to the jet force being proportional to the mass discharge rate:

$$F_{jet}(t) = v_{jet}\dot{m}(t) \tag{7}$$

By combining (4) and (7), we find a simple equation to estimate the total eject mass ($m_{total} = \int \dot{m}\, dt$):

$$m_{\text{total}} = K_0 / v_{\text{jet}} \tag{8}$$

We consider the possible range of jet velocities between 200 and 570 m/s, as suggested by Brodsky et al. (1999) to estimate the total mass shown in Figure 3b. In particular, the estimation based on the lower bound of v_{jet} is: $m_{\text{total}} \approx 6.5 \times 10^{12}$ kg. Based on this mass estimation, we compute the Hunga Tonga eruption magnitude (Mason et al., 2004) as $M = 5.8$.

The next step is to use an average tephra density (ρ_{tephra}) to convert the erupted mass into volume:

$$V_{\text{total}} = m_{\text{total}} / \rho_{\text{tephra}} \tag{9}$$

As discussed in the introduction, while the VEI may depend on several parameters, it is mainly a discrete scale logarithmically related to ejecta volume (Table 1 from Newhall & Self, 1982 and Equation 3 from Pyle, 1995). Its continuous equivalent can be written as a following equation:

$$VEI = \log\left(V_{\text{total}}/10^9\right) + 5 \tag{10}$$

where v_{total} is the volume in m^3. A final relationship between v_{total} and VEI can be written as:

$$VEI = \log\left(K_0 / v_{\text{jet}} / \rho_{\text{tephra}}\right) - 4 \tag{11}$$

Based on our estimation of K_0 from the broadband seismograms and with using $v_{jet} = 200$ m/s (Brodsky et al., 1999) and $\rho_{\text{tephra}} = 1{,}000$ kg/m^3 (Takarada & Hoshizumi, 2020), we obtain the value of VEI of 5.8 for the Hunga Tonga eruption. This estimation is subject to various uncertainties. Some of them are related to poorly known values of v_{jet} and ρ_{tephra}. So far, the latter can vary strongly depending on the composition of the ejecta and the compactness of the volcanic deposit (Mason et al., 2004).

2. Discussion and Conclusions

We first show how the continuous analysis of long period wavefield at global scale, can help to rapidly identify and locate signals different from regular earthquakes (Figures 1 and 2). Our algorithm, which is inspired on previous works (Shearer, 1994 and Ekström, 2006), permitted the rapid identification and characterization of the Hunga Tonga eruption.

We then used the seismic waves emitted from the source to get first order-dynamic parameters for this eruption. From the detected signals (Figure 2a), we can qualitatively infer a long (~6,000 s) eruption episode, dominated by a series of explosions, similar to the Mt St. Helens 1980 eruption (Brodsky et al., 1999; Kanamori & Given, 1982). With a simple spectral ratio method (Nishimura, 1995) we estimated the broadband amplitude source force spectrum (Figure 3a). The source force spectrum at low-frequencies, stabilizes at a "plateau", whose level is equal to the VEIm K_0, or the integral of the vertical force in time, and takes values of 1.3×10^{15} Ns. This value is ~2.5 times larger than the estimate of Kanamori and Given (1982) for the Mount St Helens eruption (Figure 3a), which was however a horizontal force associated with the initial blast. From the estimated explosion impulse, and assuming an explosion model (Brodsky et al., 1999), we obtain an estimate of the total eject mass of 6.5×10^{12} kg for a jet velocity of 200 m/s (Equation 4), which is significantly larger than the $1.6–4.6 \times 10^{11}$ kg, estimated by Brodsky et al. (1999) for the mount St Helens eruption in 1980.

From the analysis of the shape of the force spectrum we observe a fall-off above the corner frequency $fc \approx 0.005$ Hz. Corner frequencies have been observed for smaller volcanic explosions (Nishimura, 1995), and can be interpreted to be inversely proportional to the duration of the explosion. For the Hunga Tonga eruption, the ~200 s duration, is likely to reflect the time extent of each explosion occurring during first 6,000 s of the eruption.

The compilation of f_c for several small eruptions, shows a scaling relationship between force and duration of the explosion (Nishimura, 1995; Cruz-Atienza et al., 2001; Zobin et al., 2009). For single explosion force, and the scaling of Zobin et al. (2009) we would expect the duration of ~200 s for the force of Hunga Tonga explosion, which agrees with the observed $F_c \sim 0.005$ Hz (Figure 3a). Our estimated duration is longer (~200 s) then ~75 s estimated by Kanamori et al. (1984) for the Mt St Helens eruption, using a similar approach. From the duration of the latter eruption (Kanamori & Given, 1982), Brodsky estimated a mass discharge rate of ~2–6e9 kg/s. With our estimates, we obtain significantly larger discharge rate, up to 6.5e10 kg/s, for the Hunga Tonga eruption. However, the time window for the analysis is 6,000 s, thus assuming the volume is ejected along the analyzed window, and we obtain a mass discharge of ~2.1e9kg/s, more similar to the results of Brodsky et al. (1999).

We further observe how the force spectrum (Figure 2a) stops to decay at ~0.008 Hz, where a second plateau is observed, before an additional corner frequency at ~0.04 Hz, well seen form P waves (Figure 3a). This shape might be controlled by the eruption dynamics, and could imply explosions of variable force and duration. To test this hypothesis, we estimated the force for only the first impulse (1,000 s time window for surface waves, Figure S4 in Supporting Information S1). This first part of the eruption lacks the long period and large amplitude force (Figure 2a) and results in K_0 approximately 10 times smaller than the one for the 6,000 s window, but still capture the large size of the explosion with a VEI up to 5.

We further relate the estimates discussed above with the VEI, making limited assumptions. Our analysis shows that the Hunga Tonga eruption has VEI ≈ 6, much larger than previous explosion at this volcano (Vaughan & Webley, 2010, VEI = 2, from satellite data), and making it among the biggest volcanic eruption ever recorded with modern geophysical instrumentation. Our seismology based estimate of VEI suggests that the Hunga Tonga eruption had a similar size as the one of Pinatubo in 1991, while based on the satellite based measurements of the eruptive plume height the Hunga Tonga explosion could be even more violent (e.g., 58 vs. 35 km; https://earthobservatory.nasa.gov/images/149474/tonga-volcano-plume-reached-the-%20mesosphere).

An important approximation that we implemented for simplicity and robustness of the analysis is that we assume the total force being only vertical (neglecting the horizontal components). Any contribution of horizontal force will result in the underestimation of the total force, resulting in a reduced estimate of the total mass. However, assuming any horizontal force as large as 40% of the vertical force (Cruz-Atienza et al., 2001; Kanamori & Given, 1982), the final difference will be as small as ~10%. Another possible source of uncertainty is the limited signal-to-noise ratio of seismic signals at very low frequencies that might result in underestimation of the level of the low-frequency spectral plateau. Moreover, we observe the importance of selecting an appropriate time

window, to resolve the full source spectrum (Figure 3). With these different sources of uncertainties in mind, the presented value of K_0 should be considered as a lower-bound estimation.

To conclude, we presented a simple framework to rapidly detect and characterize remote and large volcanic explosions from the sole seismological data. The analysis of the data does not require huge computations and can be done in near real time. Nevertheless, for routine implementation of our method, more research and interdisciplinary approaches will be needed, to automatically distinguishing signals associated with volcanic explosions, from the ones generated by more frequent earthquakes, or others physical processes as landslides or large movements of ice masses (Poli, 2019; Shearer, 1994; Ekström, 2006).

We show, however, that for identified eruptions, the described approach based on a limited set of assumptions and the easily available seismological observations can be used for a rapid (within an hour) quantitative estimation of explosion sizes (e.g., VEI). The application of this approach to the Hunga Tonga eruption suggest that it had VEI of 6.

Data Availability Statement

Seismological data and Green's function are available through the IRIS Data Management Center (IRISDMC) at http://service.iris.edu/fdsnws/dataselect/1/and can be obtained using the IRIS DMC FDSNWS web service.

Acknowledgments
PP and NS received funding from the European Research Council (ERC) under the European Union Horizon 2020 Research and Innovation Programme (Grant Agreements, 802777-MONI-FAULTS and 787399-SEISMAZE, respectively). The comments from two anonymous reviewer and John J. Sanchez have helped to improve the quality of this work.

References

Albuquerque Seismological Laboratory (ASL)/USGS. (1988). Global Seismograph network - IRIS/USGS[Dataset]. International Federation of Digital Seismograph Networks. https://doi.org/10.7914/SN/IU

Allstadt, K. (2013). Extracting source characteristics and dynamics of the August 2010 Mount Meager landslide from broadband seismograms. *Journal of Geophysical Research: Earth Surface, 118*, (*3*), 1472–1490. https://doi.org/10.1002/jgrf.20110

Brodsky, E. E., Kanamori, H., & Bradford, S. (1999). A seismically constrained mass discharge rate for the initiation of the May 18, 1980 Mount St. Helens eruption. *Journal of Geophysical Research*, *104B12*, 29387–29400. https://doi.org/10.1029/1999jb900308

Brune, J. N. (1970). Tectonic stress and the spectra of seismic shear waves from earthquakes. *Journal of Geophysical Research*, *75*(26), 4997–5009. https://doi.org/10.1029/JB075i026p04997

Cruz-Atienza, V. M., Pacheco, J. F., Singh, S. K., Shapiro, C., Valdés, C., & Iglesias, A. (2001). Size of Popocatépetl volcano explosions (1997–2001) from waveform inversion. *Geophysical Research Letters*, *28*, 4027–4030.

Duncombe, J. (2022). The surprising reach of Tonga's giant atmospheric waves. *Eos*, *103*. https://doi.org/10.1029/2022eo220050

Dziewonski, A. M., & Anderson, D. L. (1981). Preliminary reference Earth model. *Physics of the Earth and Planetary Interiors*, *254*, 297–356. https://doi.org/10.1016/0031-9201(81)90046-7

Ekström, G. (2006). Global detection and location of seismic sources by using surface waves. *Bulletin of the Seismological Society of America*, *964A*, 1201–1212.

Fee, D., Izbekov, P., Kim, K., Yokoo, A., Lopez, T., Prata, F., et al. (2017). Eruption mass estimation using infrasound waveform inversion and ash and gas measurements: Evaluation at Sakurajima Volcano, Japan. *Earth and Planetary Science Letters*, *480*, 42–52. https://doi.org/10.1016/j.epsl.2017.09.043

GEOFON Data Centre. (1993). *GEOFON seismic network. Deutsches GeoForschungsZentrum GFZ*. https://doi.org/10.14470/TR560404

Global Volcanism Program. (2013). *Volcanoes of the world, v. 4.7.6*. In E.Venzke (Ed.). Smithsonian Institution. https://doi.org/10.5479/si.GVP.VOTW4-2013

Haney, M. M., Matoza, R., Fee, D., & Aldridge, D. F. (2018). Seismic equivalents of volcanic jet scaling laws and multipoles in acoustics. *Geophysical Journal International*, *213*(1), 623–636. https://doi.org/10.1093/gji/ggx554

Hutko, A. R., Bahavar, M., Trabant, C., Weekly, R. T., Van Fossen, M., & Ahern, T. (2017). Data products at the IRIS-DMC: Growth and usage. *Seismological Research Letters*, *88*(3), 892–903. https://doi.org/10.1785/0220160190

Institutde physique du globe de Paris (IPGP), École et Observatoire des Sciences de la Terre de Strasbourg (EOST). (1982). *GEOSCOPE, French Global Network of broad band seismic stations*. Institut de physique du globe de Paris (IPGP). https://doi.org/10.18715/GEOSCOPE.G

Kanamori, H., & Given, J. W. (1982). Analysis of long-period seismic waves excited by the May 18, 1980, eruption of Mount St. Helens—a terrestrial monopole? *Journal of Geophysical Research*, *87*(B7), 5422–5432. https://doi.org/10.1029/jb087ib07p05422

Kanamori, H., Given, J. W., & Lay, T. (1984). Analysis of seismic body waves excited by the Mount St. Helens eruption of May 18, 1980. *Journal of Geophysical Research: Solid Earth*, *89*(B3), 1856–1866. https://doi.org/10.1029/jb089ib03p01856

Le Pichon, A., Blanc, E., Drob, D., Lambotte, S., Dessa, J. X., Lardy, M., et al. (2005). Infrasound monitoring of volcanoes to probe high-altitude winds. *Journal of Geophysical Research*, *110*, D13106. https://doi.org/10.1029/2004JD005587

Manta, F., Occhipinti, G., Hill, E. M., Perttu, A., Assink, J., & Taisne, B. (2021). Correlation between GNSS-TEC and eruption magnitude supports the use of ionospheric sensing to complement volcanic hazard assessment. *Journal of Geophysical Research: Solid Earth*, *126*, e2020JB020726. https://doi.org/10.1029/2020jb020726

Mason, B. G., Pyle, D. M., & Oppenheimer, C. (2004). The size and frequency of the largest explosive eruptions on Earth. *Bulletin of Volcanology*, *66*, 735–748. https://doi.org/10.1007/s00445-004-0355-9

Matoza, R. S., Le Pichon, A., Vergoz, J., Herry, P., Lalande, J. M., Lee, H. I., et al. (2011). Infrasonic observations of the June 2009 Sarychev Peak eruption, Kuril Islands: Implications for infrasonic monitoring of remote explosive volcanism. *Journal of Volcanology and Geothermal Research*, *200*(1–2), 35–48. https://doi.org/10.1016/j.jvolgeores.2010.11.022

Newhall, C. G., & Self, S. (1982). The volcanic explosivity index (VEI) an estimate of explosive magnitude for historical volcanism. *Journal of Geophysical Research*, *87*(C2), 1231–1238. https://doi.org/10.1029/JC087iC02p01231

Nishimura, T. (1995). Source parameters of the volcanic eruption earthquakes at Mount Tokachi, Hokkaido, Japan, and a magma ascending model. *Journal of Geophysical Research: Solid Earth*, *100*(B7), 12465–12473. https://doi.org/10.1029/95jb00867

Poli, P. (2019). In between known earthquakes: Characteristics long period earthquakes from oceanic ridges and ultra-low frequency volcanic tremors. *Geophysical Research Abstracts*, *21*.

Prejean, S. G., & Brodsky, E. E. (2011). Volcanic plume height measured by seismic waves based on a mechanical model. *Journal of Geophysical Research*, *116*, B01306. https://doi.org/10.1029/2010JB007620

Pyle, D. M. (1995). Mass and energy budgets of explosive volcanic eruptions. *Geophysical Research Letters*, *5*, 563–566. https://doi.org/10.1029/95GL00052

Scripps Institution of Oceanography. (1986). Global Seismograph Network - IRIS/IDA [Data set]. International Federation of Digital Seismograph Networks. https://doi.org/10.7914/SN/II

Shearer, P. M. (1994). Global seismic event detection using a matched filter on long-period seismograms. *Journal of Geophysical Research*, *99*(B7), 13713–13725. https://doi.org/10.1029/94jb00498

Storchak, D. A., Di Giacomo, D., Bondár, I., Engdahl, E. R., Harris, J., Lee, W. H., et al. (2013). Public release of the ISC–GEM global instrumental earthquake catalogue (1900–2009). *Seismological Research Letters*, *845*, 810–815. https://doi.org/10.1785/0220130034

Takarada, S., & Hoshizumi, H. (2020). Distribution and eruptive volume of Aso-4 pyroclastic density current and tephra fall deposits, Japan: A M8 super-eruption. *Frontiers of Earth Science*, *8*. https://doi.org/10.3389/feart.2020.00170

Vaughan, R. G., & Webley, P. W. (2010). Satellite observations of a surtseyan eruption: Hunga Ha'apai, Tonga. *Journal of Volcanology and Geothermal Research*, *198*(1-2), 177–186. https://doi.org/10.1016/j.jvolgeores.2010.08.017

Whiters, M., Aster, R., Young, C., Beiriger, J., Harris, M., Moore, S., & Trujillo, J. (1998). A comparison of select trigger algorithms for automated global seismic phase and event detection. *Bulletin of the Seismological Society of America*, *88*(1), 95–106.

Zobin, V. M., Navarro, C., Reyes-Dávila, G., Orozco, J., Bretón, M., Tellez, A., et al. (2006). The methodology of quantification of volcanic explosions from broadband seismic signals and its application to the 2004–2005 explosions at Volcán de Colima, México. *Geophysical Journal International*, *167*(1), 467–478. https://doi.org/10.1111/j.1365-246X.2006.03108.x

Zobin, V. M., Reyes, G. A., Guevara, E., & Bretón, M. (2009). Scaling relationship for Vulcanian explosions derived from broadband seismic signals. *Journal of Geophysical Research*, *114*, B3. https://doi.org/10.1029/2008jb005983